

An Effect of Heat Transfer on MHD Flow of Nanofluids Rotating on Porous Disk

R. Lakshmi¹, R.Vijayakumar², A.Subashini³, M. Kanchana⁴

¹Assistant Professor, Department of Mathematics,

PSGR Krishnammal College for Women, Coimbatore – 641004, Tamil Nadu, India

²Mathematics Section, FEAT, Annamalai University, Annamalainagar – 608002, India.

Department of Mathematics, Periyar Arts College, Cuddalore, Tamil Nadu, India.

³Research scholar, Department of Mathematics,

PSGR Krishnammal College for Women, Coimbatore – 641004, Tamil Nadu, India

⁴Research scholar, Department of Mathematics,

PSGR Krishnammal College for Women, Coimbatore – 641004, Tamil Nadu, India

Corresponding author: R.Lakshmi Email:rluxmath@gmail.com

Article Info

Page Number: 2314 - 2338

Publication Issue:

Vol 71 No. 4 (2022)

Article History

Article Received: 25 March 2022

Revised: 30 April 2022

Accepted: 15 June 2022

Publication: 19 August 2022

Abstract

The unsteady viscous incompressible nanofluid flow is investigated analytically for copper water nanofluids under the effects of heat transfer and a uniform transverse magnetic field with the thermo physical properties, in which the flow is established between the non-coaxial rotations of a porous disk and a fluid at infinity. In this investigation, we consider that the studied nanofluid is electrically conducting and Hall currents are taken into account. In a special case, the present numerical solution is validated analytically and numerically with the earlier available results. The effects of major parameters on the dimensionless velocity, temperature and volumetric fraction of nanoparticles are analysed via representative profiles, whereas the skin friction factor and the heat transfer rate are estimated numerically and discussed through tabular illustrations.

Keywords: MHD Flow, Hall Effects, Nanofluids, Suction, Co-Axial Rotation, Porous Disk.

Introduction: Heat Transfer is the science that seeks to predict the energy transfer that may take place between material bodies as a result of a temperature difference. Whenever there is a temperature difference in a medium or between media, heat transfer must occur. There are basic

modes of heat transfer: conduction, convection and radiation. Heat conduction is the most common that it occurs in nature. It's the transfer of energy from the more energetic particles of a substance to the adjacent less energetic ones as a result of interactions between the particles. Fourier's law is introduced to solve the heat conduction problems. It states an empirical relationship between the conduction rate in a material and the temperature gradient in the direction of energy flow, which was proposed by Fourier in 1822. He drew a conclusion that the heat flux from heat conduction is proportional to the magnitude of temperature gradient and opposite to its direction. For a steady heat conduction process, the heat flux in x-direction could be expressed as: $q_x = -k \frac{dT}{dx}$ Where, q_x is the heat flux ($\frac{W}{m^2}$) in the positive x direction and $\frac{dT}{dx}$ is the temperature gradient ($\frac{K}{m}$) in the direction of heat flow. K is the thermal conductivity of material ($\frac{W}{mk}$) and it's a constant property Fourier's law is the basic law to solve the heat transfer problems and it could also be applied into unsteady multi-dimensional conduction problems.

The steady MHD flow of viscous incompressible electrically conducting nanofluid due to a non-coaxial rotation of a porous disk and a fluid at infinity in the presence of uniform transverse magnetic field is studied extensively. Hall Effect was first discovered in 1879 by Edwin Hebert Hall while working on his doctoral degree at the Johns Hopkins University in Baltimore, Maryland, USA. The Hall effect is the production of a voltage difference (The Hall voltage) across a current carrying conductor (in presence of Magnetic field), perpendicular to both current and the magnetic field. The effects due to Hall current become significant when the Hall parameter is high. This situation occurs as a result of high magnetic field. The above work is discussed by Kanch and Jana [6], Guria et al.[7], Ghar at al, [8,9].Das and Jana, [10]. The effects of Hall current with heat transfer are found to arise in many practical applications namely in power generators, Refrigeration coils, electric transformers and heating elements to mention few (Seth el al.) [11-12].

The study of magnetohydrodynamic (MHD) nanofluid flows has wide range of applications in engineering and science such as medicine delivery processing, cancer therapy, and tumour analysis. Due to the interaction between the magnetic field and electrically conducting fluid, the boundary layer control is affected. The semi analytical solution called homology analysis for unsteady magneto hydrodynamic (MHD) fluid flow and heat transfer of a Newtonian fluid, induced by an impulsively stretched plane surface is investigated by Kumari and Nath, [14] Prasad et al.[15] studied the influence of variable viscosity on viscoelastic magneto hydrodynamic fluid flow

and heat transfer over a stretching sheet and noticed that enhancement in the magnetic parameter tend to decrease the skin fraction at the sheet. Chamkha and Aly, [16] presented two dimensional steady MHD free convection boundary-layer flow of an incompressible nanofluid over a semi-infinite vertical permeable plate in the presence of Brownian diffusion. Turkyilmazoglu [17] analysed the effect of velocity slip on water-based nanofluid flow for four different type of nanoparticles viz. copper (Cu), silver (Ag), copper oxide (CuO), and titanium oxide (TiO₂) under the influence of magnetic field. Ibrahim and Shanker [18] analysed the heat transfer aspect of MHD nanofluid flow over a non-isothermal stretching sheet and found that for prescribed heat flux condition, increase in Lewis number results in an increment in the surface temperature. Sheikholeslami et al. [19] studied the MHD effect on natural convection heat transfer flow of Al₂O₃ water nanofluid and found that Nusselt number is an increasing function of the buoyancy ratio number but it is reversed for Lewis number and Hartmann number. Hayat et al., [20] analysed the unsteady MHD two-dimensional squeezing flow of a viscous and incompressible nanofluids restricted between two parallel walls under the influence of thermophoresis.

Nanofluids are homogeneous mixtures of solids and liquids when these solid particles are smaller than 100 nm. An innovative new class of heat transfer fluids that can be engineered by suspending nanoparticles in conventional heat transfer fluids and able to enhance significantly the thermal conductivity and convective heat transfer performance of its base fluids. The main goal of nanofluids is to achieve the highest possible thermal properties at the smallest possible concentrations by uniform dispersion and stable suspension of nanoparticles in host fluids. The first time the term nanofluid was defined in 1995, when Choi coined it while working in a research project at Argonne National Laboratory, USA.

The study of the fluid flow on the surface of rotating disk has got great attentions around the globe from the researcher's due to its many applications in practical problems. Electric power generating system, rotating machinery, corotating turbines, chemical process and computer storage, in the field of aerodynamics engineering, geothermal industry, for lubrication purposes, over the surface of rotating disk the fluid flow is widely applicable. Von Karman's [21] examined the solution of Navier stoke's equations by considering an appropriate transformation. Further, he used the fluid flow over the rotating frame for the first time. The Von Karman's problem and its solution numerically have been discussed by Cochrn [22]. Also, he used two series expansion by solving the limitation in the Von Karman's work. Sheikholeslami et al. [23] used numerical technique for

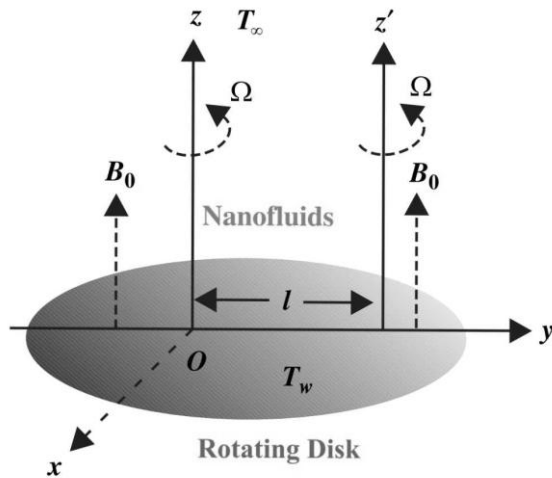
the solution of nanofluid flow over an inclined rotating disk. During the rotation of the disk, Millsaps and Pahlhauen [24] studied the heat transport characteristic. The electric field in radial direction has been considered by, Turkyilmazogu [25] where the heat transfer phenomena in magnetohydro-dynamic (MHD) fluid flow has been investigated. Under the transverse magnetic field influence, Khan et al. [26] considered the non-Newtonian Powell-Eyring fluid over the rotating disk surface. The entropy generation due to porosity of rotating disk in MHD flow has been investigated by Rashidi et al. [27]. Hayat et al [28] scrutinized the transfer of heat with viscous nanoliquid among two stretchable rotating sheets. The thermal conductivity that depends on temperature in Maxwell fluid over a rotating disk has been studied by Khan et al [28]. Bachelor [30] was the first researcher, who discussed the fluid flow between the gaps of the rotating frame. The influence of blowing with wall transpiration, suction and mixed convection has been investigated by Yan and Soong [29]. Recently Shuaib et al. [30] studied the fractional behaviour of fluid flow through a flexible rotating disk with mass and heat characteristics. The attention of researcher's is increasing towards nanofluid studies day by day due to its many applications in technology that bring facilities in many industrial process of heat transfer. The applications of nanofluid are in drugs delivery, power generation, micro manufacturing process, metallurgical sectors, and thermal therapy, etc. Choi [31] is a researcher who worked for the first time on nanofluid, where he considered it for cooling and coolant purpose in technologies. He found from his work that in a base fluid (water, oil and blood, etc.) by adding the nanoparticles, the heat transfer of thermal conductivity becomes more effective. Using the idea of Choi's idea, many researchers investigated and obtained results using the nanofluids [32,33]. A concentric circular pipe with slip flow has been discussed in Turkyilmazoglu [34]. By using finite element method (FEM), Hatami et al. [35] finds the solution for the heat transfer in nanofluid with free natural convective in a circular cavity. The Cattaner-Christov heat flux and thermal radiation for an unsteady squeezing MHD flow has been considered by Ganji and Dogonchi [36] they considered the heat of transfer of the nanofluid among two plates. Dilan et al. [37] studied nanofluids effective viscosity based on suspended nanoparticles. A carbon nanotubes based multifunctional hybrid nanoliquid has been considered by Rossella [38]. The influence of SWCNTs on human epithelial tissues is studied by Kaiser et al [39]. Hussanan et al. [40] examined the Oxide nanoparticles for the enhancement of energy in engine nanofluids, kerosene oil and water. Saeed et al. [41] examined nanofluid to

improve the heat transfer rate and reduce time for food processing in the industry. Some recent studies related to heat and mass transfer through nanofluids are examined by many researchers [42-46].

It is the aim of the present work to study the steady magnetohydrodynamic flow of a viscous incompressible electrically conducting nanofluid due to non-coaxial rotations of non-conducting porous disk and a fluid at infinity in the presence of a uniform transverse magnetic field. The disk and the fluid at infinity rotate with same angular velocity. The disk and the fluid at infinity are maintained at two different constant temperatures and the viscous dissipation and Joule heating are considered in the energy equation.

Comprehensive review on nanofluid flows have been made by Keblinski et al.[47] Wang et al.[48] Eastman et al. [49] Choi et al. [50] Buongiorno [51] and Kakac and combined with Pramuanjaroenkij [52]. Magnetohydrodynamic flow of nanofluids due to a rotating disk has numerous applications in many areas, such as rotating machinery, cooling and heating process of computer devices and crystal growth processes. In view of its wide applications in industrial and other technological fields, the problem of flow due to a rotating disk has been extended to nanofluids. Bachok et al.[53] have presented the flow and heat transfer over a rotating porous disk in a nanofluid. Rashidi et al.[54] have analyzed the entropy generation in a steady MHD flow due to a rotating porous disk in a nanofluid. Hussain et al.[55] have studied the radiative magneto-nanofluid flow over an accelerated moving ramped temperature plate with Hall effects. They have used the Laplace transform technique to solve the mathematical model and reported that the augmentation of Hall current leads to speed up the nanofluid velocity components whereas the solid volume fraction of nanoparticles has a reverse effect on it. The double diffusive MHD natural convection flow of Brinkman type nanofluid with diffusion-thermo and chemical reaction effects has been presented by Kumar et al.[54] and they solved it analytically by Laplace Transform technique.

Exact solutions are obtained for the governing equations. The numerical computations are performed using MATLAB. Effects of the pertinent parameters on the fluid velocity components, temperature, shear stresses as well as rate of heat transfer at the disk are presented graphically and tabulated.



2. Formulation of the problem and its solution:

As the temperature difference between the surface of the disk and the ambient fluid, heat transfer takes place, the energy equation with viscous dissipation and Joule heating takes the form

$$-(\rho c_p)_{nf} \omega_0 \frac{dT}{dz} = k_{nf} \frac{d^2T}{dz^2} + \mu_{nf} \left[\left(\frac{du}{dz} \right)^2 + \left(\frac{dv}{dz} \right)^2 \right] + \frac{1}{\sigma_{nf}} (J_x^2 + J_y^2) \tag{2.1}$$

where T is the temperature of the nanofluid, k_{nf} given in (2.3) and $(\rho c_p)_{nf}$ the heat capacitance of the nanofluid which is given by [1]

$$(\rho c_p)_{nf} = (1 - \phi) (\rho c_p)_f + \phi (\rho c_p)_s \tag{2.2}$$

where $(\rho c_p)_f$ the heat capacitance of the base fluid and $(\rho c_p)_s$ the heat capacitance of the nanoparticle. The first term on the right-hand side of the energy Eq. (2.1) describes heat conduction, the second term due to viscous dissipation, the third term due to the Joule heating (a volumetric heat generation due to electric resistance heating). Expressions (2.2) are restricted to spherical nanoparticles, where it does not account for other shapes of nanoparticles. The enhancement of thermal transport properties of nanofluids has been an area of intense research over the past few years. The mechanism of this enhancement has not yet been fully understood. Most of the existing theories on effective thermal properties of nanofluids are essentially derived from continuum-based phenomenological formalisms associated with pure diffusive transport mechanisms, which typically incorporate the particle shape and volume fraction as the only two independent variables [2]. Accordingly, the effective thermal conductivity of the nanofluid followed by Kakac and Pramuanjaroenkij,[3] and Oztop and Abu-Nada [4] is given by

$$k_{nf} = \frac{k_s + 2k_f - 2\phi(k_f - k_s)}{k_s + 2k_f + \phi(k_f - k_s)} \quad (2.3)$$

Where k_f is the thermal conductivity of the base fluid and k_s the thermal conductivity of the nanoparticle. The temperature boundary conditions are

$$T = T_w \text{ at } z = 0 \text{ and } T \rightarrow T_\infty \text{ as } z \rightarrow \infty \quad (2.4)$$

where T_w is the constant temperature of the surface of the disk. At large distances from the disk, T tends to T_∞ where T_∞ is the temperature of the ambient fluid.

In terms of the non-dimensional variable $(T - T_w)/(T_\infty - T_w)$ and on using [57] the consideration that the steady boundary layer flow of a nanofluid occupying the space $Z > 0$ and is bounded by an infinite porous disk at $Z = 0$. Due to the symmetry about the plane $Z = 0$, it is sufficient to consider the problem in the upper half space only. The axes of rotation of the both the disk and that of the fluid at infinity to be in the plane $x = 0$. The disk and the fluid at infinity are rotating with the same uniform angular velocity Ω about the z and z^1 axes respectively and the distance between the axes of rotation is denoted by l as depicted in Fig. 1. The disk is an electrically non-conducting and maintained at temperature T_w while the temperature of the ambient fluid is T_∞ at a large distance from the disk. A uniform transverse magnetic field \mathbf{B}_0 is applied perpendicular to the disk being subject to the disk being subject to uniform suction W_0 . The fluid is a water based nanofluid containing four types of nano particles namely copper (Cu), aluminium oxide (Al_2O_3), titanium dioxide (TiO_2) and silver (Ag). The nanoparticles are assumed to have a uniform shape and size. Moreover it is assumed that both the base fluid and nanoparticles are in thermal equilibrium state. The thermo physical properties of the nanofluid are given in Table.

The geometry of the problem suggest that the velocity field in the flow is of the form

$$\left. \begin{aligned} u = -\Omega y, v = \Omega x, w = -W_0 \quad \text{at } z = 0 \\ u = -\Omega(y - l), v = \Omega x \quad \text{at } z \rightarrow \infty \end{aligned} \right\} \quad (2.5)$$

where u, v and w are respectively the velocity components along x, y and z -direction. The boundary conditions (2.5) shows that the motion is a summation of a helical and translatory motion with the velocity field being

$$u = -\Omega y + f(z), v = \Omega x + g(z), w = h(z) \quad (2.6)$$

Thermo physical properties of water and nanoparticles.

Properties	Water/base Fluid	Cu (Copper)	Ag (Silver)	Al ₂ O ₃ (Alumina)	TiO ₂ (Titanium) Oxide
P (kg/m ³)	9997.1	8933	10500	3970	4250
c _p (J/kgK)	4179	385	235	765	686.2
K(W/mK)	0.613	401	429	40	8.9538
Φ	0.0	0.05	0.1	0.15	0.2
σ(S/m)	5.5 × 10 ⁻⁶	59.6 × 10 ⁶	-	35 × 10 ⁶	2.6 × 10 ⁶

where f, g, h, z are unknown functions and they represent the flow due to non-coaxial relations of a porous disk and a fluid at infinity.

The equation of continuity gives $\frac{\partial h}{\partial z} = 0$ which on integration yields $h = c = -\omega_0$ everywhere in the flow where $w_0 > 0$ for the suction and $w_0 < 0$ for the blowing at the disk.

On the use of 2.6, the Navier-stoke's eqns. of motion along the x, y and z-direction are

$$g\Omega = -\frac{1}{\rho_{nf}} \frac{\partial p}{\partial x} + \Omega^2 x + W_0 \frac{df}{dz} + \nu_{nf} \frac{d^2 f}{dz^2} + \frac{B_0}{\rho_{nf}} J_y \quad (2.7) \quad f\Omega = -\frac{1}{\rho_{nf}} \frac{\partial p}{\partial x} + \Omega^2 y + W_0 \frac{df}{dz} + \nu_{nf} \frac{d^2 g}{dz^2} -$$

$$\frac{B_0}{\rho_{nf}} J_x \quad (2.8)$$

$$-\frac{1}{\rho_{nf}} \frac{\partial p}{\partial z} = 0 \quad (2.9)$$

where p is the pressure of nanofluid, ν_{nf} the kinematic viscosity of the nanofluid, μ_{nf} the dynamic viscosity of the nanofluid

$$\mu_{nf} = \frac{\mu_f}{(1-\phi)^{2.5}}, \rho_{nf} = (1-\phi)\rho_f + \phi\rho_s,$$

$$\sigma_{nf} = \sigma_f \left(1 + \frac{3(\sigma-1)\phi}{(\sigma+2) - (\sigma-1)\phi} \right), \sigma = \frac{\sigma_s}{\sigma_f} \quad (2.10)$$

where ϕ is the solid volume fraction of nanoparticles ($\phi = 0$ correspond to a regular fluid), ρ_f the density of the base fluid, ρ_s the density of the nanoparticle, σ_f the electrical conductivity of the base fluid, σ_s the electrical conductivity of the nanoparticle.

The boundary condition for f and g are

$$f=0, y=0 \text{ at } z=0$$

$$f=\Omega l, g=0 \text{ as } z \rightarrow \infty \text{ for } t > 0 \quad (2.11)$$

Making reference to Cowling when the strength of the magnetic field is very large, the generalized Ohm's law is modified to include Hall current so that

$$\vec{J} + \frac{\omega_e \tau_e}{B_0} (\vec{J} \times \vec{B}) = \sigma_{nf} (\vec{E} + \vec{q} \times \vec{B})$$

where $\vec{q}, \vec{B}, \vec{E}, \vec{J}, \omega_e$ and τ_e are respectively the velocity vector, the magnetic field vector, the electric field vector, cyclotron frequency and electron collision time.

$\nabla \cdot \mathbf{B} = 0$ (The solenoidal relation) Integrating w.r.t. y

$$B_y = \text{Constant} = \mathbf{B}_0$$

where $\mathbf{B} = (0, B_y, 0)$ (flow only in y direction).

The Conservation of electric charge is given by $\nabla \cdot \sigma = 0$.

$$\Rightarrow J_z = \text{Constants, where } \vec{J} = (J_x, J_y, J_z) \quad J_z = 0$$

The first term of the left hand side of (2.8) comes from the electron drag of the ions.

The second term represents the effects due to Hall currents and has to develop with the idea that electrons and ions can decouple and move separately. It is assumed that the magnetic Reynolds number ($Rem \leq 1$) for the flow is very small, so that induced magnetic field can be neglected in comparison with the imposed field \mathbf{B}_0 . This assumption is justified since the magnetic Reynolds number is generally very small for metallic liquid or partially ionized fluid. Liquid metals can be used in a range of applications because they are non-flammable, nontoxic environmentally safe. That is why, liquid metals have number for technical applications in source exchanges, electronic pumps, amount heat exchangers and also used as a heat engine fluid. Moreover in nuclear power plants sodium, alloys, lead-bismuth and bismuth are extensively used in heat transfer process. Besides that mercury play its role as a fluid in high-temperature Rankine cycles and also used in reactors in order to reduce the temperature of the system. For power plants which are exerted at extensively high temperature, sodium is treated as a heat-engine fluid. The remaining is given in Eqn. (2.1)

$$\Rightarrow J_x + m J_y = \sigma_{nf} [E_x + v \mathbf{B}_0] \quad (2.12)$$

$$J_y - m J_x = \sigma_{nf} [E_y - u \mathbf{B}_0] \quad (2.13)$$

Where $m = \omega_e \tau_e$ stands for Hall parameter which can take positive or negative values. In general, for an electrically conducting fluid, Hall currents affect the flow in the presence of a strong magnetic field. Further it is assumed that $\omega_e \tau_e \sim o(1)$ and $\omega_i \tau_i \leq 1$, where ω_e, ω_i are the cyclotron frequencies of electrons and ions and τ_e, τ_i are the collision times of electrons and ions. In writing

the magnetic induction equation, the ion slip effects arising out of imperfect coupling between ions and neutrals as well as the electron pressure gradient are neglected. The effect of Hall currents gives rise to a force in the z-direction, which induces a cross-flow in that direction and hence the flow becomes three-dimensional. To simplify the problem, we assume that there is no variation of flow quantities in z direction.

In the free-stress, the magnetic field is uniform, so that there is no current and hence, we have

$$J_x \rightarrow 0, J_y \rightarrow 0 \text{ as } z \rightarrow \infty \quad (2.14)$$

In view of (2.14), we obtain from (2.12) and (2.13)

$$\begin{aligned} \sigma_{nf} [E_x + v \mathbf{B}_0] &= 0 \quad \sigma_{nf} E_x + \sigma_{nf} v \mathbf{B}_0 = 0 \\ \Rightarrow E_x &= -\Omega \mathbf{B}_0 x, \quad E_y = -\Omega \mathbf{B}_0 (y - 1) \end{aligned} \quad (2.15)$$

everywhere in the flow. It is known that

$$J_x + m J_y = \sigma_{nf} [-\Omega \mathbf{B}_0 x + v \mathbf{B}_0]$$

$$J_x + m J_y = \sigma_{nf} \mathbf{B}_0 [-\Omega x + v]$$

$$J_x = \sigma_{nf} \mathbf{B}_0 [-\Omega x + v] - m J_y \text{ from (2.12)}$$

$$J_y = \sigma_{nf} E_y - \sigma_{nf} u \mathbf{B}_0 + m J_x \text{ from (2.13)}$$

$$J_x = \sigma_{nf} \mathbf{B}_0 [-\Omega x + v] - m \sigma_{nf} (E_y - u \mathbf{B}_0) + m J_x \quad J_x = \sigma_{nf} \mathbf{B}_0 [-\Omega x + v] - m \sigma_{nf} E_y - m \sigma_{nf} u \mathbf{B}_0 - m^2 J_x$$

$$J_x + m^2 J_x = \sigma_{nf} \mathbf{B}_0 [m u - \Omega x + v] - m \sigma_{nf} E_y$$

$$J_x [1 + m^2] = \sigma_{nf} \mathbf{B}_0 (m u - \Omega x + v) - m \sigma_{nf} (-\Omega \mathbf{B}_0 (y - 1))$$

$$[1 + m^2] = \sigma_{nf} \mathbf{B}_0 (m u - \Omega x + v + m \sigma_y - m \Omega l)$$

$$f = u + \Omega y, \quad g = v - \Omega x$$

$$J_x [1 + m^2] = \sigma_{nf} \mathbf{B}_0 [m f + g - m \Omega l]$$

$$J_x [1 + m^2] = \sigma_{nf} \mathbf{B}_0 [g - m(\Omega l - f)]$$

$$J_x = \frac{\sigma_{nf}}{1 + m^2} [g - m(\Omega l - f)] \quad (2.16)$$

$$J_y = \sigma_{nf}(E_y - uB_0) + m J_x$$

$$J_y = \sigma_{nf}[-\Omega B_0(y-1) - B_0u] + \frac{m\sigma_{nf}B_0}{1+m^2}[g- m(\Omega l - f)]$$

$$J_y = -\Omega B_0y\sigma_{nf} + \Omega B_0l \sigma_{nf} + \frac{m\sigma_{nf}B_0}{1+m^2}g - \frac{m\sigma_{nf}B_0}{1+m^2}(\Omega l f)$$

$$J_y = -B_0\sigma_{nf}[u + \Omega y] + \Omega B_0l \sigma_{nf} + \frac{m}{1+m^2} \sigma_{nf}B_0[g- m(\Omega l - f)]$$

$$= -B_0\sigma_{nf} + B_0\sigma_{nf} \Omega l + \frac{m}{1+m^2} \sigma_{nf}B_0[g- m(\Omega l - f)]$$

$$= \frac{[(1+m^2)(\Omega l - f) + mg - m^2(\Omega l - f)]B_0\sigma_{nf}}{(1+m^2)}$$

$$J_y = \frac{B_0\sigma_{nf}}{(1+m^2)}[mg + (\Omega l - f)] \quad (2.17)$$

Substituting equation (2.16) & (2.17) in equation (2.7) to (2.9)

$$-g\Omega = \Omega^2 x + \frac{1}{\rho_{nf}} \frac{\partial f}{\partial x} + \omega_0 \frac{\partial f}{\partial z} v_{nf} \frac{\partial^2 f}{\partial z^2} + \frac{\sigma_{nf} B_0^2}{\rho_{nf}(1+m^2)} [(\Omega l - f) + mg] \quad (2.18)$$

$$-f\Omega = -\Omega^2 y + \frac{1}{\rho_{nf}} \frac{\partial p}{\partial y} + \omega_0 \frac{\partial f}{\partial z} v_{nf} \frac{\partial^2 g}{\partial z^2} - \frac{\sigma_{nf} B_0^2}{\rho_{nf}(1+m^2)} [g- m(\Omega l - f)] \quad (2.19)$$

$$-\frac{1}{\rho_{nf}} \frac{\partial p}{\partial z} = 0 \quad (2.20)$$

on the use of infinity Conditions, equation (2.18) & (2.19) yield

$$g = 0, f = \Omega l \text{ as } z \rightarrow \infty$$

now the equations (2.18) & (2.19) becomes

$$0 = -\Omega^2 x + \frac{1}{\rho_{nf}} \frac{\partial p}{\partial z} \quad (2.21)$$

$$-\Omega^2 l = -\Omega^2 y + \frac{1}{\rho_{nf}} \frac{\partial p}{\partial z} \quad (2.22)$$

$$-g \Omega = \omega_0 \frac{\partial f}{\partial z} + v_{nf} \frac{\partial^2 f}{\partial z^2} + \frac{\sigma_{nf} B_0^2}{\rho_{nf}(1+m^2)} [(\Omega l - f) + mg]$$

$$\Rightarrow v_{nf} \frac{\partial^2 f}{\partial z^2} + \omega_0 \frac{\partial f}{\partial z} + \Omega g + \frac{\sigma_{nf} B_0^2}{\rho_{nf}(1+m^2)} [(\Omega l - f) + mg]$$

(2.23) Similarly,

$$v_{nf} \frac{\partial^2 f}{\partial z^2} + \omega_0 \frac{\partial f}{\partial z} - \Omega^2 l + f\Omega - \frac{\sigma_{nf} B_0^2}{\rho_{nf}(1+m^2)} [g- m(\Omega l - f)] = 0 \quad (2.24)$$

Now combining equation (2.23) & (2.24), (2.23) + (2.24)

$$v_{nf} \left(\frac{\partial^2 f}{\partial z^2} + \frac{\partial^2 g}{\partial z^2} \right) + \omega_0 \left(\frac{\partial f}{\partial z} + \frac{\partial g}{\partial z} \right) + \Omega [g + \Omega l - k] + \frac{\sigma_{nf} B_0^2}{\rho_{nf} (1+m^2)} [(\Omega l - f) + mg] - [g + m(\Omega l - f)] = 0 \quad (2.25)$$

Introducing upon non- dimensional variables $\eta = \sqrt{\frac{\Omega}{\nu_f}} z, F = 1 - \left[\frac{f}{\Omega l} + i \frac{g}{\Omega l} \right]$

any $\eta \rightarrow 0$ (ie) $v_{nf} = \nu_f$

$$i = \sqrt{-1} \sqrt{2} = \sqrt{\frac{1}{2^8}} \quad (2.26)$$

$$f + ig = (1 - F) \Omega l$$

$$= \frac{1}{2\sqrt{2}} = -\frac{1}{2} 2^{-\frac{3}{2}}$$

and combining (2.23) and (2.24)

$$\left(\frac{\nu_f}{\Omega l} \frac{\partial^2 f}{\partial z^2} \right) \left(\frac{\omega_0}{\Omega l} \cdot \frac{\partial F}{\partial z} \right) + \Omega [\Omega l - (f - g)]$$

$$x_2 \frac{\partial^2 f}{\partial \eta^2} + x_1 \frac{\partial F}{\partial \eta} \left(\frac{x_3 M^2}{1+m^2} + \left(i x_1 + \frac{x_3 m M^2}{1+m^2} \right) \right) F = 0 \quad (2.27)$$

where

$$\left. \begin{aligned} x_1 &= \left[(1 - \varphi) + \varphi \left(\frac{\rho_s}{\rho_f} \right) \right], \quad x_2 = \frac{1}{1 - \varphi^{2.5}}, \\ x_3 &= \left[1 + \frac{3(\sigma - 1)\varphi}{(\sigma + 2) - (\sigma - 1)\varphi} \right] \sigma = \frac{\sigma_s}{\sigma_f} \end{aligned} \right\} \quad (2.28)$$

and $M^2 = \frac{\sigma_f B_0^2}{(\rho_f \Omega)}$ is the magnetic parameter which represents the ratio of the magnetic force to the viscous force and $\varepsilon = \frac{\omega_0}{\sqrt{\Omega \nu_f}}$ the suction/blowing parameter. The boundary conditions for $F(\eta)$ are

$$F(0) = 1 \quad \text{and} \quad F \rightarrow 0 \quad \text{as} \quad \eta \rightarrow \infty$$

Solution of (2.27) subject to boundary conditions (2.28) can easily be obtained and on using (2.26), we get

$$\frac{f}{\Omega l} = 1 - e^{-\alpha^* \eta} \cos \beta \eta \quad \text{and} \quad (2.29)$$

$$\frac{g}{\Omega l} = e^{-\alpha^* \eta} \sin \beta \eta \quad (2.30)$$

On using (2.11) and (2.12) the Eq. (2.1) takes the form

$$x_5 \frac{d^2 \theta}{d \eta^2} + x_4 \operatorname{spr} \frac{d \theta}{d \eta} = \operatorname{prEc} \left[x_2 (\alpha^{*2} + \beta^2) + \frac{x_3 M^2}{1+m^2} \right] e^{-2\alpha^* \eta} \quad (2.31)$$

Where $x_4 = \left[(1 - \phi) + \phi \frac{(\rho c_p)_s}{(\rho c_p)_f} \right]$,

$$x_5 = \left[\frac{k_s + 2k_f - 2\phi(k_f - k_s)}{k_s + 2k_f + \phi(k_f - k_s)} \right] \quad (2.32)$$

where x_1, x_2, x_3 are given by

$$x_1 = \left[(1 - \phi) + \phi \left(\frac{\rho_s}{\rho_f} \right) \right], \quad x_2 = \frac{1}{1 - \phi^{2.5}},$$

$$x_3 = \left[1 + \frac{3(\sigma - 1)\phi}{(\sigma + 2) - (\sigma - 1)\phi} \right] \sigma = \frac{\sigma_s}{\sigma_f} \quad (2.33)$$

α^*, β are given by

$$\alpha, \beta = \frac{1}{2\sqrt{2}x_2} \left[(a_1^2 + b_1^2)^{\frac{1}{2}} \pm a \right]^{\frac{1}{2}}, \quad \alpha^* = \left(\frac{\epsilon x_1}{2x_2} + \alpha \right),$$

$$a = \left(\epsilon^2 x_1^2 + \frac{4x_2 x_3 M^2}{1 + m^2} \right),$$

$$b = 4x_2 \left(x_1 + \frac{mM^2 x_3}{1 + m^2} \right) \quad (2.34)$$



and $Pr = \frac{(\mu c_p)_f}{k_f}$ is the Prandtl number which measures the ratio of momentum diffusivity to the thermal diffusivity, $Ec = \Omega^2 l^2 / ((c_p)_f)(T_w - T_\infty)$ the Eckert number signifying the ratio of kinetic energy of the flow to the boundary layer enthalpy difference. Since $T_w > T_\infty$, Ec is positive which shows that heat transfer phenomenon is taking place from disk to the fluid.

$Ec = 0$ corresponds to no Joule and viscous heatings.

The corresponding boundary conditions for $\theta(\eta)$ are

$$\theta(0) = 0 \text{ and } \theta(\infty) = 1 \quad (2.35)$$

Solution of (2.30) subject to the boundary conditions (2.34) is

$$\theta(\eta) = 1 - e^{-\delta\eta} + \frac{prEc \left[x_2(\alpha^{*2} + \beta^2) + \frac{x_3 M^2}{1 + m^2} \right]}{2x_5 \alpha^* (2\alpha^* - \delta)} x (e^{-2\alpha^* \eta} - e^{-\delta\eta}) \text{ for } \delta \neq 2\alpha^*$$

$$1 - e^{-\delta\eta} - \frac{prEc \left[x_2(\alpha^{*2} + \beta^2) + \frac{x_3 M^2}{1 + m^2} \right]}{\delta} x \eta e^{-\delta\eta} \text{ for } \delta = 2\alpha^* \quad (2.36)$$

Where $\delta = x_4 SPr/x_5$, α^* and β are given by (2.34). Solution (2.36) is valid only for suction ($S > 0$) at the disk. We point out that no steady distribution of temperature exists for injection at the disk. From a physical point of view, this is due to the fact that the temperature at a given point is continuously raised due to conduction of heat away from the disk and convection of heat away from the disk due to injection. If $\phi = 0$ (correspond to pure water), the solution (2.36) coincides with solutions (2.4) and (2.31) of Guria et al [5] in a substitution of $x_1 = 0$,

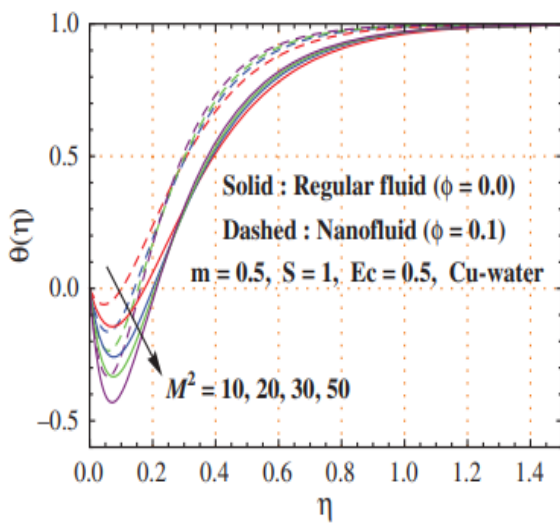
$y_1 = 1$.

Solution (2.34) exhibits a thermal boundary layer double deck structure for $\delta \neq 2\alpha^*$. The thickness of these layers are of order $O(\delta^{-1})$ and $O(1/2)\alpha^{*-1}$. On the other hand, for $\delta = 2\alpha^*$ there is a single-deck thermal boundary layer with thickness of order of $O(\delta^{-1})$. It is interesting to observe from the expression of that this thickness is not affected by the magnetic parameter M^2 and Hall parameter m , but depends solely on the suction parameter S and volume fraction ϕ of nanoparticles for fixed values of Pr .

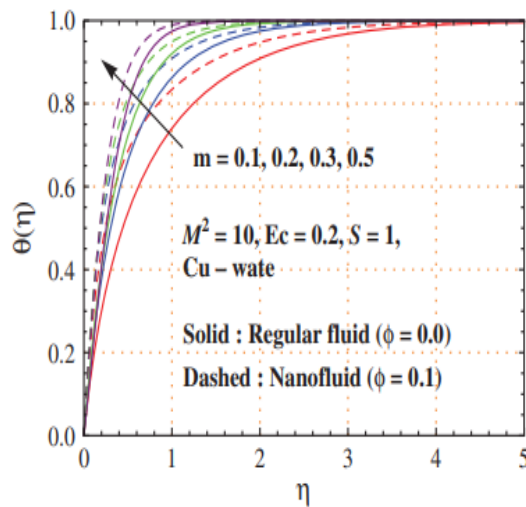
2.1. Effects of parameter on Temperature profiles

Figure 1 has been sketched to analyse the effects of magnetic parameter M^2 , Hall parameter m , suction parameter S , Eckert number Ec and solid volume fraction ϕ on the temperature profile. Figure 1(a) exhibits the impact of M^2 on the temperature profiles. It is seen that with an increase in M^2 , there is a decrease in the fluid temperature for the region < 0.29 and then it increases. This can be explained by the fact that due to enhancement of magnetic field strength, a resistive type force called Lorentz force has the tendency to slow down the fluid motion. The fluid layer is not enough warmer under the influence of magnetic force. Thus, the fluid temperature decreases near disk when the magnetic field strength becomes stronger. When the magnetic parameter M^2 increases, the fluid temperature function becomes negative near disk. Such an effect does not seem in the absence of the magnetic field. In addition, it should be noted that there is no such an effect of the magnetic parameter M^2 for a pure water ($\phi = 0$). The variation of fluid temperature with an increase in Hall parameter m can be shown in Figure 1(b). Temperature increases due to the increase of m as a result of fluid velocity increase which increases the viscous dissipation and hence the fluid temperature. Figure 1(c) illustrates the variations of fluid temperature with respect to suction parameter S . This figure depicts that the fluid temperature increases when the values of S increases. This is due to the fact that the fluid is brought closer to the plate surface and reduces the thermal boundary layer thickness. The effect of Eckert number Ec on the fluid temperature is shown in Figure 1(d). It is evident from the figure that as Ec increases the fluid temperature is increased. An increase in Eckert number results in the increase in dissipation effects which leads to a rise in the fluid temperature. Figure 1(e) describes the effect of nanoparticle volume fraction on the fluid temperature. It is seen that with an increase in ϕ , there is a decrease in $\Theta(\eta)$. It indicates that the addition of nanoparticles reduces the temperature of pure water by a considerable amount. This observation justifies the use

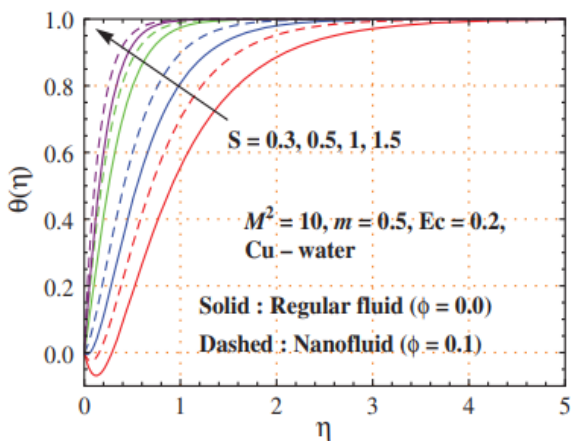
of nanoparticles as coolants in several engineering applications. Also, the thermal boundary layer thickness increases, as the nanoparticle volume fraction increases. This issue is in compliance with the primary purpose of employing nanofluids. From Figures 1(a)–(d), it can be observed that the Cu-water nanofluid ($\phi = 0.1$) has the largest temperature profiles and pure water ($\phi = 0$) has the smallest one. This is because of the higher thermal conductivity of the Cu-water nanofluid compared with that of pure water. This observation justifies the use of nanoparticles as coolant in several engineering applications.



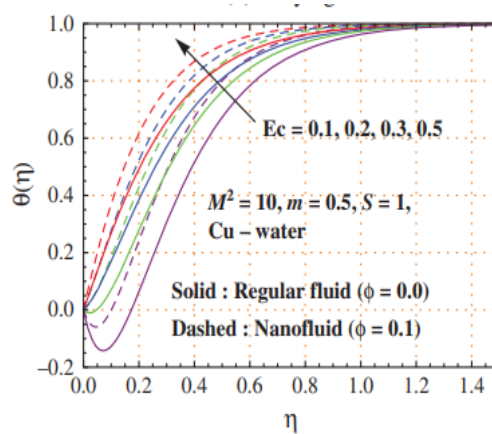
(a) Varying M^2



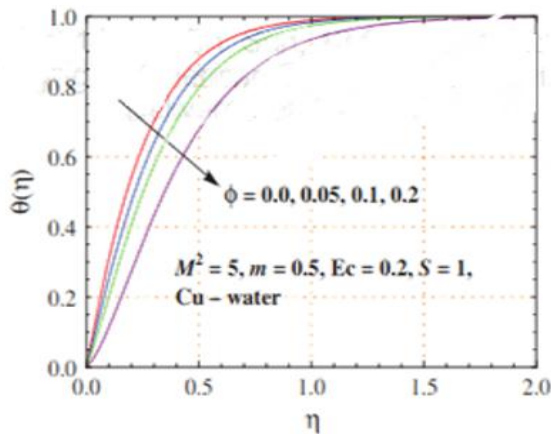
(b) Varying m



(c) Varying S



(d) Varying Ec



(e) Varying time φ

Fig.1. Variations in temperature profiles for increasing values of embedded parameters.

2.2 Effects of Parameters on Rate of Heat Transfer

The rate of heat transfer at the disk $\eta = 0$ is given by

$$\begin{aligned} \Theta'(0) &= \left(\frac{d\theta}{d\eta} \right)_{\eta=0} \\ &= \delta - \frac{\text{prEc}}{x_5 \delta} \left[x_2 (\alpha^{*2} + \beta^2) + \frac{x_3 M^2}{1+m^2} \right] \end{aligned} \quad (2.36)$$

where x_2, x_3 are given by (2.33), x_5 is given by (2.33), and α^*, β^* are given by (2.34)

Numerical results of the rate of heat transfer $\Theta'(0)$ at the plate $\eta = 0$ are presented in Figure 8 for several values of M^2, m, S, Ec and ϕ . It is noted that the rate of heat transfer $\Theta'(0)$ is lowest with Cu followed by Al_2O_3 and TiO_2 while Ag produced the highest rate of heat transfer as shown in Figure 2(a). This is due to the fact that the Cu has the largest value of thermal diffusivity which leads to reduction in the temperature gradient. Figure 2(b) depicts that as M^2 increases, $\Theta'(0)$ decreases. This is due to the fact that increasing M^2 resists the flow velocity towards the disk and then prevents the fluid at near-ambient temperature to be brought to the neighborhood of the surface of the disk which reduces the heat transfer. Furthermore, $\Theta'(0)$ is an increasing function of m . Figures 2(c) and (d) present the variations of the rate of heat transfer $\Theta'(0)$ with respect to S and Ec . It is seen that the rate of heat transfer $\Theta'(0)$ increases for increasing values of S whereas it decreases with increase in Ec . Figure 2(e) shows that the rate of heat transfer $\Theta'(0)$ decreases when ϕ becomes larger. This indicates that an increase in volume fraction of copper nanoparticles results in additional enhancement of the heat transfer rate at the disk. This is due to the enhanced thermal conductivity of nanofluid attained by the addition of copper nanoparticles. This enhanced thermal conductivity facilitates the heat transfer between the fluid and disk surface. On the other hand, $\Theta'(0) > 0$ means

the heat flows from the ambient fluid to the disk. This is not surprising since the fluid is hotter than the disk.

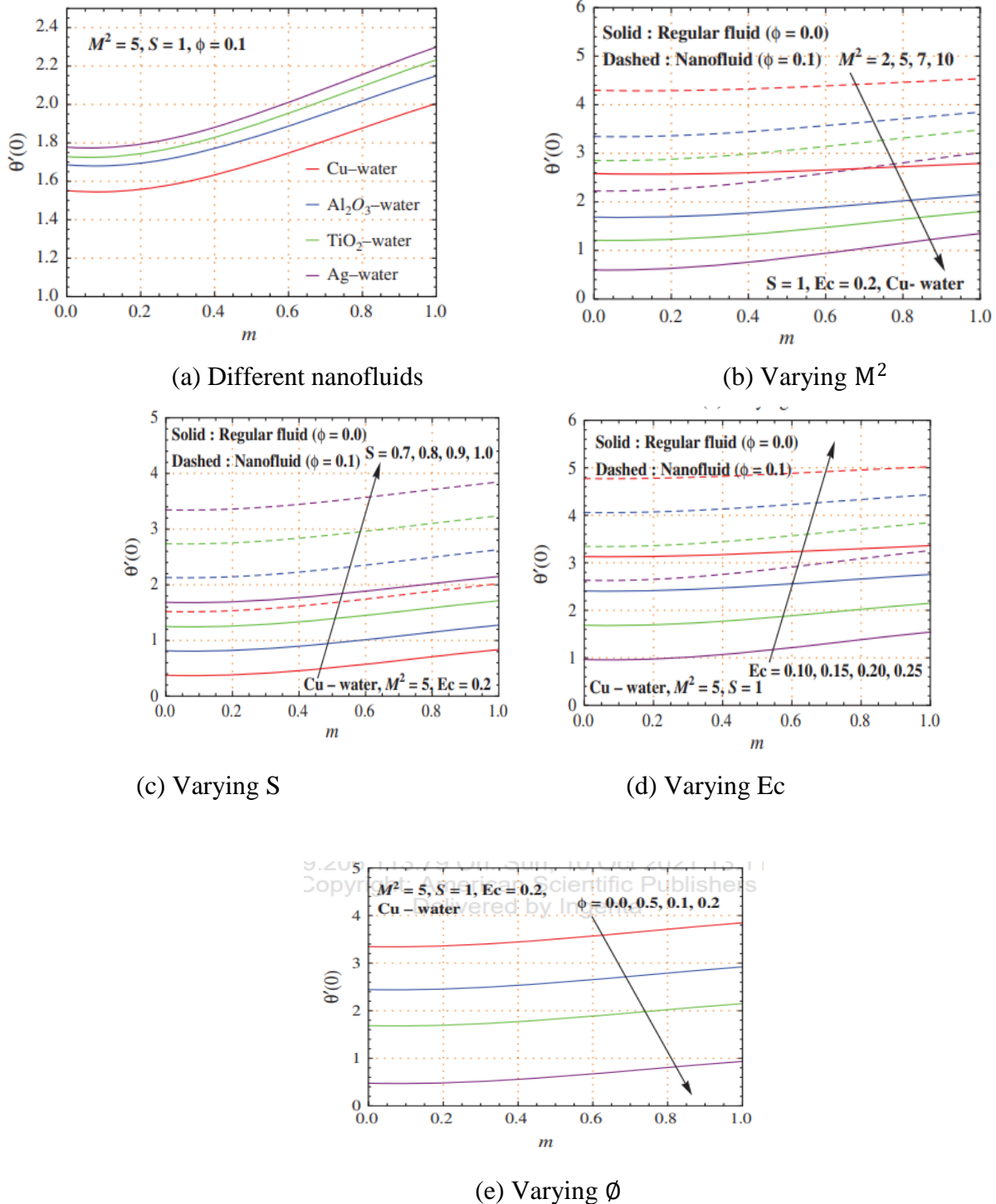


Fig 2. Variations heat transfer $\Theta'(0)$ for increasing values of embedded parameters.

2.3 Critical Eckert Number:

It is seen from (2.31) that when $Ec = Ec^*$ where

$$Ec^* = \frac{2x_4 S \alpha^*}{\left[x_2 (\alpha^{*2} + \beta^2) + \frac{x_3 M^2}{1+m^2} \right]} \quad (2.37)$$

x_2, x_3 given by (2.33), x_4 given by (2.32) and α^*, β given by (2.33), there will be no flow of heat either from the disk to the fluid or fluid to the disk. We have computed the numerical values of critical Eckert number Ec^* for various values of M^2, m, S and ϕ in Figure 3. The variation of critical Eckert number Ec^* is demonstrated in Figure 3(a) for four types of water-based nanofluids Cu-water, Al_2O_3 -water, TiO_2 -water and Ag-water.

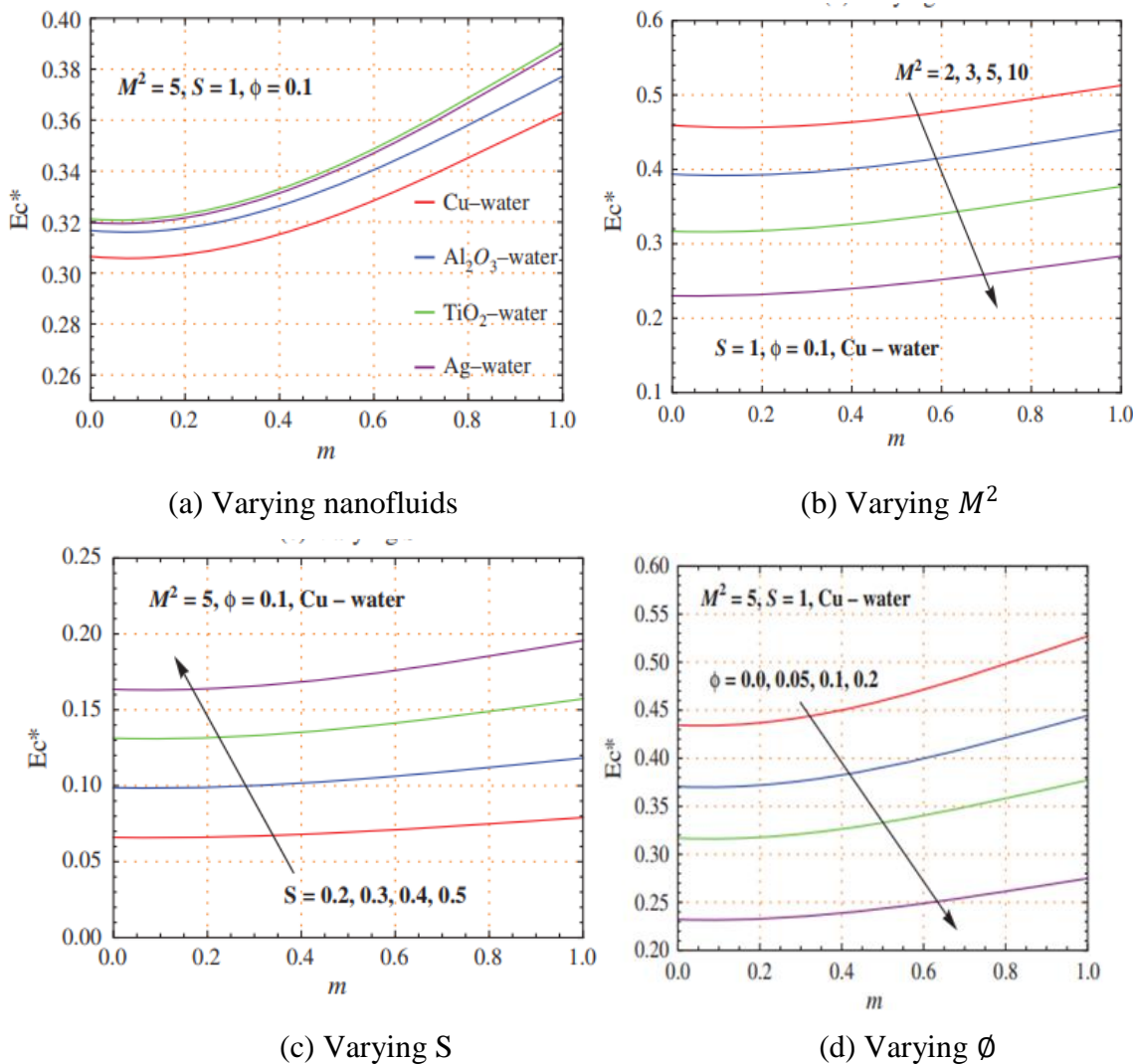


Fig.3. Variations of critical Eckert number Ec^* for increasing values of embedded parameters.

2.4 Matlab Coding:

```

z=linspace(0,1.4,100);
phi=0.1;
rho_f=997.1;
rho_s=8933;
s1=0.0000055;
s2=59600000;
sigma=s1/s2;
cp_f=4179;
cp_s=385;
ks=401;
kf=0.613;
S=1;
M=50;
m=0.5;
S1=2;
Pr=1;
Ec=0.5;
x1=(1-phi)+phi*(rho_s/rho_f);
x2=1/((1-phi)^(2.5));
x3=(1+((3*(sigma-1)*phi)/((sigma+2)-(sigma-1)*phi)));
x4=1-phi+phi*((rho_s*cp_s)/(rho_f*cp_f));
x5=(ks+2*kf-2*phi*(kf-ks))/(ks+2*kf+phi*(kf-ks));
d=(x4*S*Pr)/x5;
a=S^2*x1^2+((4*x2*x3*M)/(1+m^2));
b=4*x2*(x1+((m*M*x3)/(1+m^2)));
p=(1/2*(sqrt(2))*x2)*(((a^2+b^2)^(1/2))+a)^(1/2);%alpha
q=(1/2*(sqrt(2))*x2)*(((a^2+b^2)^(1/2))-a)^(1/2);%beta
r=((S*x1)/(2*x2))+p;%alpha*
r1=(-(S1*x1)/(2*x2))+p;%alpha_1*
if d==2*r1

```

```

theta=1-exp(-d*z)-((Pr*Ec*(x2*(r1^2+q^2)+x3*M/(1+m^2)))/d)*z*exp(-d*z);
else if
theta=1-exp(-d*z)+((Pr*Ec*(x2*(r1^2+q^2)+(x3*M)/(1+m^2)))/(2*x5*r1*(2*r1-d)))*(exp(-
2*r1*z)-exp(-d*z));
end
plot(z,theta)
hold on

```

3. Result and discussion:

It is observed that the critical Eckert number Ec^* is lowest for the Cu-water nanofluid than Al_2O_3 -water, TiO_2 -water nanofluids and Ag-water. It is observed from Figures 3(c)–(d) that the critical Eckert number decreases with an increase in either M^2 or while it increases for increasing values of S . Further, the critical Eckert number Ec^* is an increasing function of Hall parameter m . The heat may flow from the fluid to the disk for $Ec > Ec^*$ even if the temperature of the disk is greater than that of the free-stream temperature, i.e., $T_w > T_\infty$. The reversal of heat flow can be explained on physical ground. It is seen that if there is significant viscous dissipation near the disk then the temperature of the fluid near the disk may exceed the disk temperature. This will cause the flow of heat from the fluid to the disk even though $T_w > T_\infty$, since we have not only taken viscous dissipation into account but also include the Joule dissipation of heat and hence there is a strong reason for the heat to flow from fluid to the disk under certain conditions.

Conclusion:

The effects of the pertinent parameters on the flow fields and the rate of heat and force exerted by the fluid on the disk have been analyzed. The important results of the present study can be listed as, increasing magnetic parameter or nanoparticle volume fraction results in an increase the components of force exerted by the fluid on the disk. A novel result of the study is that no torque is exerted on the plate by the fluid. The inclusion of viscous dissipation and Joule heating has prominent effects on the thermal boundary layer. A thermal boundary layer is formed in the vicinity of the disk. It has a thickness of an order of magnitude that is inversely proportional to either the suction parameter or nanoparticle volume fraction. The critical Eckert number is smallest for the Cu-water nanofluid than Al_2O_3 -water, TiO_2 water and Ag-water nanofluids.

Reference:

- [1] X. Xuan and D. Li, *J. Micromech. Microeng.* 14, 1171 (2004).
- [2] P. Keblinski, S. R. Phillpot, S. U. S. Choi, and J. A. Eastman, *Int. J. Heat Mass Transf.* 45, 855 (2002).
- [3] S. Kakaç and A. Pramuanjaroenkij, *Int. J. Heat Mass Transf.* 52, 3187 (2009)
- [4] H.F. Oztop and E.Abu-Nada. *Int. J. Heat Fluid Flow* 29, 1326 (2008)
- [5] M. Guria, B. K. Das, and R. N. Jana, *Int. J. Fluid Mech. Res.* 34, 535 (2007).
- [6] Kanch A. K. and Jana R. N., *Rev. Roum. Sci. Techn.* 39, 619 (1997).
- [7] Guria M, Das S and. Jana R. N, *Int. J. Non-Linear Mech.* 42, 1204 (2007).
- [8] Ghara N, Guria M and Jana R. N, *Meccanica* 47, 557 (2012).
- [7] Ghara N, Das S, Maji S. L and Jana R. N, *J. Mech.* 29, 337 (2013).
- [8] Das S and Jana R. N, *Ain Shams Eng. J.* 5, 1325 (2014).
- [9] Seth G. S, Nandkeolyar R, Mahto N, and Singh S. K, *Int. J. Theo. Appl. Mech.* 4, 205 (2009).
- [10] Setha G. S and Singh J. K, *Appl. Math. Modeling* 40, 2783 (2016).
- [11] Seth G. S, Sarkar S and Makinde O. D. *J. Mech.* 32, 613 (2016).
- [12] Kumari M and Nath G, *Commun. Nonlinear Sci. Numer. Simul.* 14, 3339 (2009).
- [13] Prasad K. V, Pal D, Umesh V and Rao N. S. P, *Commun. Nonlinear Sci. Numer. Simul.* 15, 331 (2010)
- [14] Chamkha A. J and Aly A.M, *Chem. Eng. Comm.* 198, 425 (2011).
- [15] Turkyilmazoglu M, *Chem. Eng. Sci.* 84, 182 (2012).
- [16] Ibrahim W and Shankar B, *Comput J, Fluids* 75, 1 (2013).
- [17] Sheikholeslami M, Gorji-Bandpy M, Ganji D. D, Rana P and Soleimani S, *Comput. Fluids* 94, 147 (2014).
- [18] Hayat T, Muhammad T, Qayyum A, Alsaedi A, and Mustafa M, *J. Molecular Liquids* 213, 179 (2016).
- [19] Von Kármán, Uber T. laminar and turbulent Reibung. *Angew Z. Math. Mech.* 1, 233–252 (1921).
- [20] Cochran, W. G. The flow due to a rotating disc. In *Mathematical Proceedings of the Cambridge Philosophical Society*, Vol. 30, No. 3. 365–375 (Cambridge University Press, 1934).

- [21] Sheikholeslami, M., Hatami, M. & Ganji, D. D. Numerical investigation of nanofluid spraying on an inclined rotating disk for cooling process. *J. Mol. Liq.* 211, 577–583 (2015).
- [22] Millsaps, K. & Pohlhausen, K. Heat transfer by laminar flow from a rotating plate. *J. Aeronaut. Sci.* 19(2), 120–126 (1952).
- [23] Turkyilmazoglu, M. Effects of uniform radial electric field on the MHD heat and fluid flow due to a rotating disk. *Int. J. Eng. Sci.* 51, 233–240 (2012).
- [24] Khan, N. A., Aziz, S. & Khan, N. A. MHD flow of Powell-Eyring fluid over a rotating disk. *J. Taiwan Inst. Chem. Eng.* 45(6), 2859–2867 (2014).
- [25] Rashidi, M. M., Kavyani, N. & Abelman, S. Investigation of entropy generation in MHD and slip flow over a rotating porous disk with variable properties. *Int. J. Heat Mass Transf.* 70, 892–917 (2014).
- [26] Hayat, T., Nazar, H., Imtiaz, M. & Alsaedi, A. Darcy-Forchheimer flows of copper and silver water nanofluids between two rotating stretchable disks. *Appl. Math. Mech.* 38(12), 1663–1678 (2017).
- [27] Khan, M., Ahmed, J. & Ahmad, L. Application of modified Fourier law in von Kármán swirling flow of Maxwell fluid with chemically reactive species. *J. Braz. Soc.*
- [28] Batchelor, G. K. Note on a class of solutions of the Navier-Stokes equations representing steady rotationally-symmetric flow. *Q. J. Mech. Appl. Math.* 4(1), 29–41 (1951).
- [29] Yan, W. M. & Soong, C. Y. Mixed convection flow and heat transfer between two co-rotating porous disks with wall transpiration. *Int. J. Heat Mass Transf.* 40(4), 773–784, (1997).
- [30] Shuaib, M., Bilal, M., Khan, M. A. & Malebary, S. J. Fractional analysis of viscous fluid flow with heat and mass transfer over a flexible rotating disk. *Comput. Model. Eng. Sci.* 123(1), 377–400 (2020).
- [31] Choi, S. U. & Eastman, J. A. Enhancing thermal conductivity of fluids with nanoparticles (No. ANL/MSD/CP-84938; CONF951135–29). Argonne National
- [32] Buongiorno, J. Convective transport in nanofluids (2006).
- [33] Kuznetsov, A. & Nield, D. A. Double-diffusive natural convective boundary-layer flow of a nanofluid past a vertical plate. *Int. J. Therm. Sci.* 50(5), 712–717 (2011).
- [34] Turkyilmazoglu, M. Anomalous heat transfer enhancement by slip due to nanofluids in circular concentric pipes. *Int. J. Heat Mass Transf.* 85, 609–614 (2015).

- [35] Hatami, M., Song, D. & Jing, D. Optimization of a circular-wavy cavity filled by nanofluid under the natural convection heat transfer condition. *Int. J. Heat Mass Transf.* 98, 758–767 (2016).
- [36] Dogonchi, A. S. & Ganji, D. D. Investigation of MHDnanofluid flow and heat transfer in a stretching/shrinking convergent/ divergent channel considering thermal radiation. *J. Mol. Liq.* 220, 592–603 (2016).
- [37] Udawattha, D. S., Narayana, M. & Wijayarathne, U. P. Predicting the effective viscosity of nanofluids based on the rheology of suspensions of solid particles. *J. King Saud Univ. Sci.* 31(3), 412–426 (2019).
- [38] Arrigo, R., Bellavia, S., Gambarotti, C., Dintcheva, N. T. & Carroccio, S. Carbon nanotubes-based nanohybrids for multifunctional nanocomposites. *J. King Saud Univ. Sci.* 29(4), 502–509 (2017).
- [39] Kaiser, J. P., Buerki-Turnherr, T. & Wick, P. Influence of single walled carbon nanotubes at subtoxic concentrations on cell adhesion and other cell parameters of human epithelial cells. *J. King Saud Univ. Sci.* 25(1), 15–27 (2013)
- [40] Hussanan, A., Salleh, M. Z., Khan, I. & Shafe, S. Convection heat transfer in micropolar nanofluids with oxide nanoparticles in water, kerosene and engine oil. *J. Mol. Liq.* 1(229), 482–488 (2017).
- [41] Salari, S. & Jafari, S. M. Application of nanofluids for thermal processing of food products. *Trends Food Sci. Technol.* (2020).
- [42] Naqvi, S. M. R. S., Muhammad, T. & Asma, M. Hydromagnetic flow of Cassonnanofluid over a porous stretching cylinder with Newtonian heat and mass conditions. *Phys. A Stat. Mech. Appl.* 123988 (2020).
- [43] Sohail, M. & Naz, R. (2020). Modified heat and mass transmission models in the magnetohydrodynamic flow of Sutterbynanofluid in stretching cylinder. *Phys. A Stat. Mech. Appl.* 124088.
- [44] Xu, C., Xu, S., Wei, S. & Chen, P. Experimental investigation of heat transfer for pulsating flow of GPs-water nanofluid in a microchannel. *Int. Commun. Heat Mass Transfer* 110, 104403 (2020).

- [45] Reddy, P. S. & Sreedevi, P. Impact of chemical reaction and double stratification on heat and mass transfer characteristics of nanofluid flow over porous stretching sheet with thermal radiation. *Int. J. Ambient Energy* 1–26 (just-accepted) (2020).
- [46]. Rafique, K., Anwar, M. I., Misiran, M., Khan, I. & Sherif, E. S. M. The implicit Keller box scheme for combined heat and mass transfer of Brinkman-type micropolar nanofluid with Brownian motion and thermophoretic effect over an inclined surface. *Appl. Sci.* 10(1), 280 (2020).
- [47] Keblinski P, Phillpot S.R, Choi S.U.S, and Eastman J.A, *Int. J. Heat Mass Transf.* 45, 855 (2002).
- [48] Wang X, Xu X and Choi S.U.S, *Thermophys J. Heat Transf.* 13, 474 (1999).
- [49] Eastman J.A, Choi S.U.S, Li S, Yu W, and Thompson L.J, *Appl. Phys. Lett.* 78, 718 (2001).
- [50] Choi S.U.S, Zhang Z.G, Yu W, Lockwood F.E, and Grulke E.A, *Appl. Phys. Lett.* 79, 2252 (2001).
- [51] Buongiorno J, *ASME J. Heat Transf.* 128, 240 (2006).
- [52] Kakaç S and Pramuanjaroenkij A, *Int. J. Heat Mass Transf.* 52, 3187 (2009).
- [53] Bachok N, Ishak A, and Pop I, *Phys. B* 406, 1767 (2011).
- [54] Rashidi M.M, Abelman S, and Freidoni N Mehr, *Int. J. Heat and Mass Transf.* 62, 515 (2013).
- [55] Hussain S.M, Sharma R, Mishra M.K, and G. Seth S, *J. Nanofluids* 6, 840 (2017).
- [56] Kumar A, Singh R, Seth G.S, and Tripathi R, *J. Nanofluids* 7, 33 (2018).
- [57] Das S, Tarafdar B and Jana R.N. *Journal of Nanofluids* Vol 7, pp.1172-1186, 2018.

About Authors :

1)



R.Lakshmi

Assistant Professor, Department of Mathematics,

PSGR Krishnammal College for Women, Coimbatore – 641004, Tamil Nadu, India

2)



R. Vijayakumar

Mathematics Section, FEAT, Annamalai University, Annamalai Nagar – 608002, India.

Department of Mathematics, Periyar Arts College, Cuddalore, Tamil Nadu, India.

3)



A. Subashini

Research scholar, Department of Mathematics,

PSGR Krishnammal College for Women, Coimbatore – 641004, Tamil Nadu, India

4)



M Kanchana

Research scholar, Department of Mathematics,

PSGR Krishnammal College for Women, Coimbatore – 641004, Tamil Nadu, India